Proceedings of 5th Jagiellonian Symposium on Advances in Particle Physics and Medicine, Kraków, Poland, 2024

Formation of Long-Lived Nuclear Molecules in (p, ^{2}He) Nuclear Reactions on ^{159}Tb and ^{181}Ta

I.M. Kadenko[a,b,*], B.M. Bondar[c], N.V. Sakhno[a,b], A.O. Didik[b], B. Biró[d] and A. Fenyvesi[d]

[a]*International Nuclear Safety Center of Ukraine, Taras Shevchenko National University of Kyiv, Volodymyrska St., 64/13, 01601 Kyiv, Ukraine*
[b]*Department of Nuclear and High Energy Physics, Faculty of Physics, Taras Shevchenko National University of Kyiv, Volodymyrska St., 64/13, 01601 Kyiv, Ukraine*
[c]*Radiopharmaceutical Production Department, Clinical Hospital "Feofaniya", Zabolotnogo St., 21, 03143 Kyiv, Ukraine*
[d]*HUN-REN Institute for Nuclear Research (HUN-REN ATOMKI), Bem tér 18/c, H-4026 Debrecen, Hungary*

Doi: 10.12693/APhysPolA.146.709 *e-mail: imkadenko@univ.kiev.ua

This paper deals with the study of long-lived nuclear molecules, consisting of heavy nuclei — products of the (p, ^{2}He) nuclear reactions on ^{159}Tb and ^{181}Ta — and ^{2}He in a bound state. The lighter nucleus ^{2}He is localised within the potential well of a heavy one, but both of them keep their identity and constitute an equivalent nucleus of the atom, which does not recognise the complex structure of such a nuclear molecule. We identified this unique configuration based on processing results of instrumental gamma-ray spectra of Tb and Ta foil samples irradiated with protons of energies below the thresholds of the corresponding (p, $2p$) nuclear reaction. Then we experimentally determined the half-lives of ^{2}He decaying by positron emission and electron capture for the Fermi and Gamow–Teller transitions and calculated the phase space factors as well as the binding energy and the radius of ^{2}He to be equal 402 keV and 10.2 fm, respectively.

topics: electron capture (EC) and positron decay, diproton bound nucleus, binding energy, radius of diproton

1. Introduction

We continued our study dedicated to two- and identical nucleon bound systems [1–3] and considered atomic-nuclear structure, in which two nuclei can be located at a few fm distances and keep their identities for a long time (from the nuclear point of view). To some extent, such configurations are similar to nuclear molecules [4], for the first time experimentally introduced in 1960 in heavy-ion nuclear physics. Such molecules represented a system that consists of two nuclei bound together on their surface in a quasi-molecular potential, i.e., a configuration of two touching nuclei which keep their individuality before flying apart or coalescing into a fused nucleus [4]. From this definition, the following features are important for our consideration:

- two nuclei,
- overlapping potential wells,
- both nuclei keeping their individuality till flying apart or fused.

In our case, two nuclei — a heavy one and ^{2}He, or diproton — moved apart at a greater distance, although still within the range of the strong interaction. In other words, to get ^{2}He bound, it must be located within the potential well of a heavy nucleus, but out of its radius range. Therein, both nuclei keep their individuality, not being recognized by the atom to which they belong. Once formed, such configurations can manifest their properties by nuclear decay of at least one of two nuclei. Then, there is an opportunity to study these nuclear properties in order to clearly identify such a unique nuclear structure and derive its extremely important characteristics before two nuclei with atomic masses A and 2 fly apart or fuse in the $A+2$ nucleus. This is the subject of this paper.

2. Experimental setup

For the experiment, we utilized the MGC-20E cyclotron of HUN-REN ATOMKI to accelerate protons up to 6.0 MeV for Tb sample irradiation and

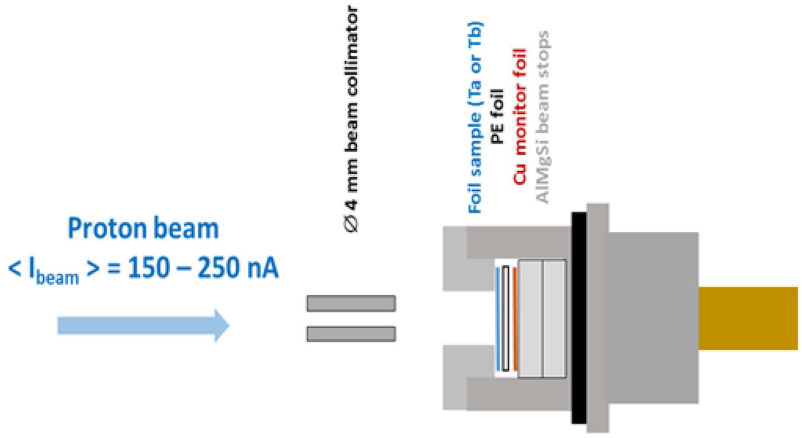

Fig. 1. The experimental setup for proton irradiation of Tb and Ta samples.

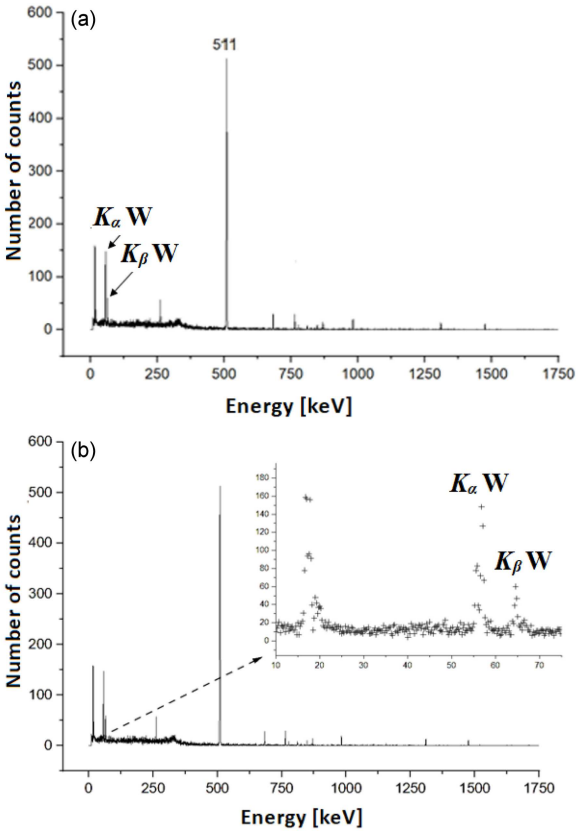

Fig. 2. The instrumental spectrum of (a) ^{181}Ta sample after 5.8 MeV proton irradiation with (b) zoom in low energy region of interest.

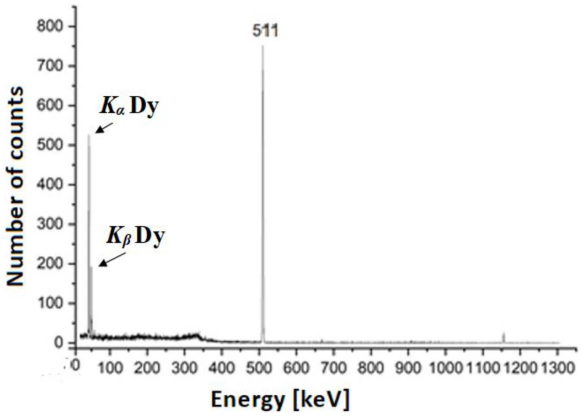

Fig. 3. The instrumental spectrum of ^{159}Tb sample after 6.0 MeV proton irradiation.

up to 5.8 MeV for Ta sample irradiation. The sketch of the irradiation unit is presented in Fig. 1 with all the main details needed to form a 4 mm diameter proton beam spot on Ta and Tb foils.

This unit was installed inside the vacuum system. Two sequential irradiations of the Ta sample with dimensions of $\sim$ 10 mm $\times$ 10 mm $\times$ 90 μm were carried out for 60 and 90 min. Then, the Ta sample was transferred to a high-purity germanium (HPGe) spectrometer for cyclic measurements of 100 s live time each. A similar procedure was applied to the Tb sample. Typical gamma spectra measured for the Ta and Tb samples are presented in Figs. 2 and 3, respectively.

The spectra include three main peak structures: K_α and K_β series of W and Dy, respectively, and very intensive peaks of 511 keV in both spectra caused by the annihilation of positrons due to decay of ^{2}He in a bound state into the deuteron, positron, and electron neutrino.

3. Experimental data

After processing all instrumental spectra acquired with a Mirion Canberra GX2018 type vertical XtRa HPGe detector equipped with an iPA-SL preamplifier used with negative output polarity, we obtained three sets of peak count rates, i.e., for K_α series and K_β series without deconvolution of peaks and for 511 keV annihilation peak. Then, each of

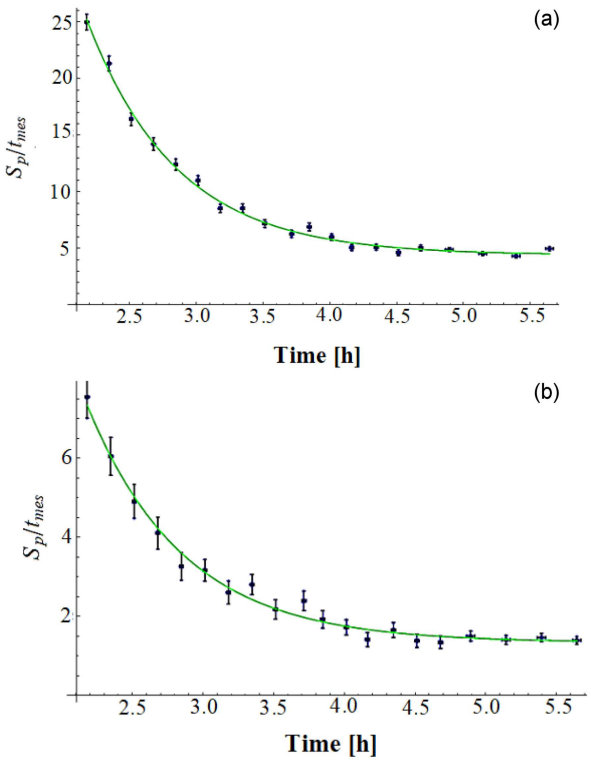

Fig. 4. Experimental data and fitting results of count rates in peaks of characteristic radiation for K_α (a) and K_β (b) series of W for Ta irradiated sample.

TABLE I

Half-lives derived from the fitting of peak count rates for Ta and Tb samples.

$T_{1/2}$ for Ta sample [h]	$T_{1/2}$ for Tb sample [h]
W-K_α: 0.49 ± 0.05	Dy-K_α: 0.47 ± 0.02
W-K_β: 0.42 ± 0.07	Dy-K_β: 0.47 ± 0.03
511 keV: 0.46 ± 0.01	511 keV: 0.48 ± 0.01

these sets was fitted with one exponential function. As the most expected open reaction channel corresponds to the (p, n) nuclear reaction, then for the Ta sample after proton irradiation the characteristic peaks of K_α and K_β series of W due to ^{181}Ta (p, n) ^{181}W nuclear reaction, as well as K_α and K_β series of Dy due to ^{159}Tb(p, n) ^{159}Dy nuclear reaction, for Tb sample after irradiation with protons must be present in the instrumental spectra. This is exactly what we have to observe with the following expected half-lives: 121.2 days for ^{181}W and 144.4 days for ^{159}Dy. The graphical results and fitting parameters of half-lives that were derived from the full set of instrumental spectra for the Ta sample are presented in Figs. 4 and 5. For all three fittings, the χ^2 per degree of freedom (d.o.f.) was less than 2.5.

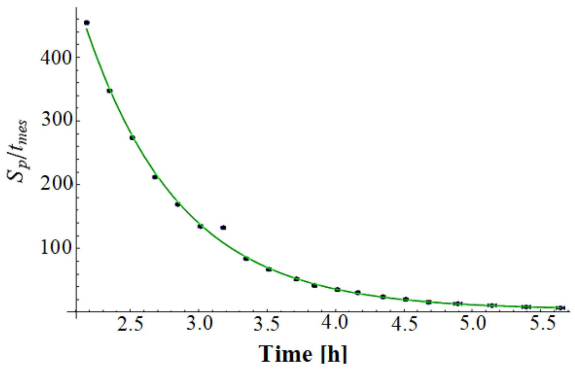

Fig. 5. Experimental data and fitting results of count rates in 511 keV peak.

TABLE II

Energies of the characteristic peaks of W.

	Energy [keV]	Intensity [%]
XR $K_{\alpha 2}$	56.28	18.7
XR $K_{\alpha 1}$	57.535	32
XR $K_{\beta 3}$	64.948	3.6
XR $K_{\beta 1}$	65.222	7.0
XR $K_{\beta 2}$	66.982	2.4

Table I presents half-lives estimated from decay curve fits with the exponential function of data sets for Ta and Tb samples. In Table II, we provided a list of characteristic peak energies for K_α and K_β series of W.

As one can see from the fitting results, the prevailing contributor to K_α and K_β series peaks, as well as 511 keV peak count rates, is independent of sample materials and can represent one out of two, but the same reaction product for both nuclear reactions. It manifests its properties via electron capture (EC) and positron decay modes with the same half-life that is essentially different from expected ones for ^{181}W and ^{159}Dy decays. However, both of these (p, n) reaction products are only EC decays.

As we assumed above, the following nuclear reactions take place:

- ^{181}Ta (p,^{2}He)^{180}Hf

and

- ^{159}Tb (p,^{2}He)^{158}Gd.

Both heavy nuclei in the output channels are stable, and in the case of ^{180}Hf, its isomeric state [5] is not excited due to the excitation energy of less than 1.1 MeV. Therefore, the only nuclear process that can be used to explain our results is the formation of a bound ^{2}He nucleus in the output channel. Then this nucleus (^{2}He) decays via EC or β^+-decay mode, capturing electrons from the K shell of W and Dy atoms (K_α and K_β series peaks) or emitting a positron, which annihilates afterwards (511 keV peak).

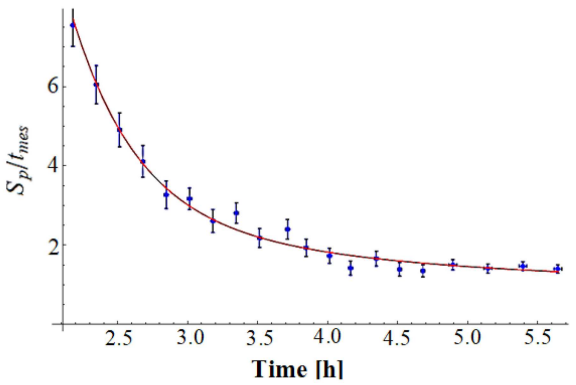

Fig. 6. Approximation by the exponent of K_β series peak for Ta sample.

TABLE III

Half-lives for Ta spectrum according to (1).

Half-life	$T^1_{1/2}$ [s]	$T^2_{1/2}$ [s]
K_α series	$1\,256 \pm 79$	$4\,439 \pm 407$
K_β series	$1\,120 \pm 119$	$5\,555 \pm 2\,038$
511 keV	$1\,220 \pm 65$	$4\,438 \pm 1\,224$

In [3], we assumed that there could be two possible ways for ^{2}He to decay into the deuteron, positron, and electron neutrino, i.e., via the Gamow–Teller transition to form the deuteron in a triplet bound state, or via the Fermi transition to form the deuteron in a singlet bound state. Even though the last one was known as rather impossible to exist, the mechanism of binding two nucleons in a singlet state, described in [6], may be realized for the deuteron as well. Based on our earlier results, we decided to fit the same data set for Ta (Fig. 4) with the sum of three exponential functions:

$$f(t) = A_1 \exp\left(-\frac{\ln(2)}{T^1_{1/2}}t\right) + A_2 \exp\left(-\frac{\ln(2)\ t}{T^2_{1/2}}\right) + A_3 \exp\left(-\frac{\ln(2)\,t}{T^3_{1/2}}\right). \quad (1)$$

In this expression, the first term corresponds to the decay of ^{2}He via the Gamow–Teller transition, the second one — to the decay of ^{2}He via the Fermi transition, and the third one — to the EC decay of ^{181}W. As an example, in Fig. 6, one can see the fitting results of the same experimental set of peak count rates with three exponential functions.

Numerical results of experimental data fits are summarized in Table III. Also, the half-life values derived for the K_α and K_β series are given in Table III. For 511 keV count rates vs time fitting, we used only two terms in (1), namely the first and the second.

These half-life estimates are in good agreement with our previous results, namely $T^{1*}_{1/2} = 1\,140 \pm 216$ s for the Gamow–Teller transition and $T^{2*}_{1/2} = 5\,516 \pm 1\,030$ s for the Fermi transition obtained only for 511 keV peaks processing [3]. It is then clear that a bound ^{2}He mainly decays into the triplet state of the deuteron and the Fermi transition is less likely, which corresponds to much greater uncertainty of its half-life for all three sets of experimental data.

As soon as we obtained the experimental estimates of both half-lives, it became possible to calculate the phase space factor f using Eq.(3) of [3]. For the Gamow–Teller transition, we get the following value $f = 0.474$, and then numerically solving the semi-empirical equation from the original book [7] or Eq.(4) of [3] relative to the endpoint energy of the positron decay spectrum, we finally obtain the following value $E_{\beta+\max} = 0.529$ MeV. Now, using the same algorithm as was described in [3], we may get the value of the binding energy of ^{2}He nucleus in a bound state as follows: $B_{dp} = 0.402$ MeV. This value of the binding energy is also in good agreement with our assumption (guess) in [3], i.e., $B_{dp} = 0.384$ MeV. Finally, taking Eq.(2) from [3], we come up with a new estimate of the radius for a bound ^{2}He nucleus, $r_{dp} \approx 10.2$ fm.

4. Discussion

If we would like to imagine the configuration of a nuclear molecule as a result of the nuclear reaction ^{181}Ta(p,^{2}He)^{180}Hf and its further transformations, then it might look as it is shown in Fig. 7. Of course, we could ask ourselves how it would be possible that such a nuclear system could exist at all taking into account a distance between two protons.

On the one hand, the distance between two protons in ^{2}He may be more than 20 fm, and the strong interaction does not certainly play any significant role in keeping both protons bound in this nucleus. On the other hand, the presence of the heavy and deformed nucleus ^{180}Hf with its potential well may stabilize ^{2}He and let it exist long enough for what was observed in our experiments. In addition, this unique configuration could probably be explained based on the results of Efimov's calculations for the case when the light particles resonate with the heavy nucleus but not with one another and then long-range interaction appears [8]. In addition, Migdal implicitly predicted in [6] the possibility of such a nuclear configuration.

Anyhow, our experimental observations and some theoretical approaches in support of what was presented above allow us to claim that we have detected ^{2}He EC and positron decays, indirectly confirming the possibility of ^{2}He co-existence in a bound state as a part of a nuclear molecule.

Should we decide to directly confirm the decay of ^{2}He not only via EC mode (K_α and K_β series) but via positron decay as well, then the instrumental positron spectrum must be recorded. It should

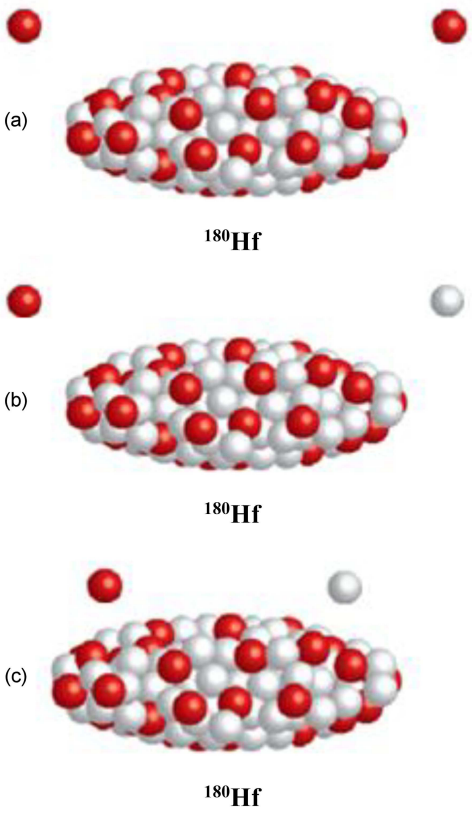

Fig. 7. Schematic representations of ^{180}Hf $+^{2}$He nuclear molecule and its transformation: (a) ^{180}Hf $+^{2}$He; (b) ^{180}Hf $+^{2}$H immediately after EC or positron decay of ^{2}He; (c) ^{180}Hf $+^{2}$H after deuteron shrinkage to its well-known radius.

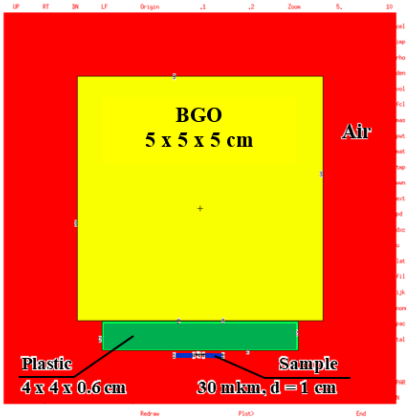

Fig. 8. Scheme of the beta–gamma spectrometer for positron spectra detection in coincidence mode.

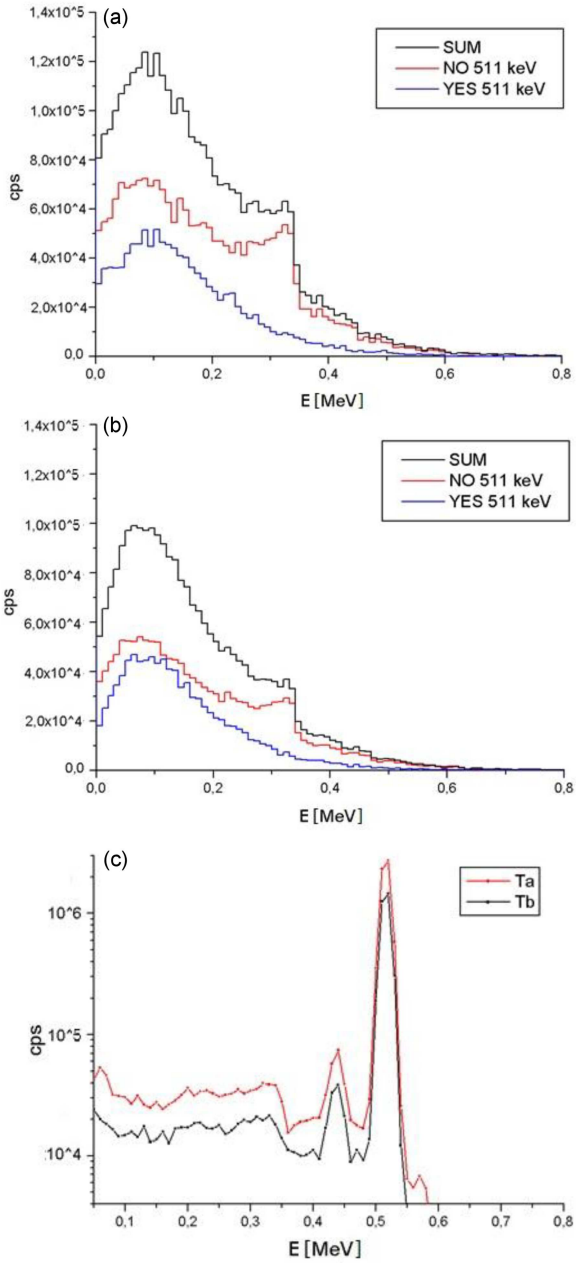

Fig. 9. Response of plastic scintillator from (a) ^{181}Ta and (b) ^{159}Tb samples and (c) response of BGO γ-detector. "NO 511 keV" means that no coincidences are taken into account, and "YES 511 keV" means that a coincidence mode is turned on.

be noted that our estimate of the limiting energy for the positron spectrum above is very important. Then, to do so, we decided to develop the Monte Carlo N-Particle eXtended (MCNPX) [9] model of the experiment, in which Ta and Tb proton irradiated samples were counted applying the simplest version of the beta–gamma spectrometer, schematically illustrated in Fig. 8.

The instrumental spectrum of positrons is to be measured by a plastic scintillator with dimensions of $4 \times 4 \times 0.6$ cm^3. In order to distinguish positron signals from the accompanying background, the coincidence mode is applied with $5 \times 5 \times 5$ cm^3 BGO (bismuth germanate) crystal detecting 511 keV gamma-rays caused by positron annihilation. Detectors are placed in close vicinity to each other, and signals from the beta-detector are recorded only in the case of energy deposition in BGO crystal within the range of 0.48–0.55 MeV. The source of positrons in

simulations is specified to be uniformly distributed along the path of protons inside the samples and limited by a beam radius of 2 mm. The thickness of samples was chosen to be 30 μm minimizing possible positron spectra distortion. The results of simulations for irradiation conditions considered in Sect. 2 are shown in Fig. 9.

The simulated spectra do not include random coincidences and show a clear positron instrumental spectrum, i.e., generated by beta plus–gamma signals within the same source-particle history. In Fig. 9, it can be seen that the intensity of positron detection is nearly the same for both samples, while the background (without coincidence with 511 keV) for ^{181}Ta is about $\sim$ 1.5 times higher. It may be caused by higher Z and density of the Ta sample, leading to attenuation of positron spectra on the sample's surface and subsequent shift of the average range of positrons inside the plastic scintillator in comparison with ^{159}Ta sample (annihilation occurs farther from the BGO crystal). The higher density of the sample also results in a greater induced activity from accompanied (p, x) reactions, enhancing the total background for both detectors. In this connection, the ^{159}Tb sample seems to be more preferable to measure the spectrum of positrons from ^{2}He decay.

5. Conclusions

In this study, we have demonstrated experimental data and provided solid evidence in support of the existence of a bound ^{2}He nucleus as a part of nuclear molecules composed of this unique He isotope and the heavy nuclei ^{180}Hf or ^{158}Gd. Both these heavy nuclei and ^{2}He in its bound state are the products of (p, ^{2}He) nuclear reaction on ^{181}Ta and ^{159}Tb, respectively. The formation of a bound ^{2}He is possible only near the surface of strongly deformed nuclei due to the requirement to set up the potential well expanding up to a distance of 2 fm the range of the strong interaction beyond the radius of the heavy nucleus. Then, two protons can be located within such a potential well to form ^{2}He, or the diproton. The very important feature of the existence of such a nuclear molecule is keeping the individuality of both ^{2}He and the heavy nucleus. In other words, with such configuration, the diproton may evince its unique nuclear properties via its EC and positron decay modes.

Both ways for ^{2}He to decay were experimentally confirmed. Moreover, we obtained the estimates of the decay half-lives, the space phase factor, the beta spectrum endpoint energy due to ^{2}He positron decay, the binding energy, and the radius of ^{2}He, which were derived from our experimental observations.

So far, the EC mode of ^{2}He was recorded in the low energy range of the instrumental gamma-spectra, and a logical continuation would be the observation of positron spectra due to β^{+}-decay of ^{2}He with the limiting energy obtained above. To address the concern of whether such an experiment would be feasible at all, we developed the simplest model of the experiment to detect positron spectra due to ^{2}He β^{+}-decay in Ta and Tb samples. As it was found, such an experiment could be reasonably designed and performed to directly observe ^{2}He positron decay using a thin Tb sample. Moreover, if the positron emission tomography (PET) technique [10–13] would be complemented to design a more sophisticated experiment with two beta and gamma-detectors, covering about the 4π geometry, then a much clearer positron spectrum could be recorded with a much higher signal to noise ratio. The statistical significance of such spectra could then be essentially improved.

Acknowledgments

The research carried out at HUN-REN ATOMKI was supported by the TKP2021-NKTA-42 project financed by the National Research, Development and Innovation Fund of the Ministry for Innovation and Technology, Hungary.

The MGC-20 cyclotron of HUN-REN ATOMKI is a Research Infrastructure of the Cluster of Low Energy Accelerators for Research (CLEAR) of the EURO-LABS project. I.M. Kadenko was supported by the Transnational Access of the CLEAR EURO-LABS project. The EURO-LABS project has received funding from the European Union's Horizon Europe Research and Innovation Programme under Grant Agreement No. 101057511.

References

[1] I. Kadenko, *Europhys. Lett.* **114**, 42001 (2016).

[2] I. Kadenko, B. Biro, A. Fenyvesi, *Europhys. Lett.* **131**, 52001 (2020).

[3] Kadenko I.M., Bondar B.M., Gorbachenko O.M., N.V. Sakhno, *Acta Phys. Pol. A* **142**(3), 337 (2022).

[4] W.Greiner, J.Y. Park, W. Scheid, *Nuclear molecules*, World scientific publishing, 1995, p. 465.

[5] NuDat 3 Data Base. National Nuclear Data Center (NNDC), Brookhaven National Laboratory, Upton, NY, USA (2023).

[6] A.B. Migdal, *Yad. Fiz.* **16**, 427 (1972) (in Russian) / *Sov. J. Nucl. Phys.* **16**, 238 (1973).

[7] G. Friedlander, J.W. Kennedy, E.S. Macias, J.M. Miller: *Nuclear and Radiochemistry*, pp. 132-138, John Wiley & Sons, Inc., USA 1981.

[8] V. Efimov, *Nuclear Physics* **A210**, 157 (1973).

[9] D.B. Pelowitz, editor. MCNPX User's Manual Version 2.6.0. Los Alamos National Laboratory. LA-CP-07-1473 (April 2008).

[10] P. Moskal, E. Czerwiński, J. Raj et al., *Nature Communications* **15**, 78 (2024).

[11] P. Moskal K. Dulski, N. Chug et al., *Science Advances* **7**, eabh4394 (2021).

[12] P. Moskal, A. Gajos, M. Mohammed et al., *Nature Communications* **12**, 5658 (2021).

[13] F.F. Ardebili, S. Niedźwiecki, P. Moskal, *Bio-Algorithms and Med-Systems* **19**, 132 (2023).